Proceedings of the 28th IEEE
EMBS Annual International Conference
New York City, USA, Aug 30-Sept 3, 2006



# Analysis of corneal images for the recognition of nerve structures

Alfredo Ruggeri, Fabio Scarpa, Enrico Grisan

*Abstract*— **The recognition of nerve structures in the cornea appears to be an important clinical issue, e.g. to investigate about damages from surgical interventions (LASIK/PRK) or severity of diabetic neuropathy. We addressed the problem of recognizing and tracing corneal nerves in confocal microscopy images. After image luminosity and contrast are normalized, the nerve tracking procedure is run. After nerve segments are recognized, a post-processing procedure removes false recognitions and links sparse segments. A prototype of the algorithm was implemented in the Matlab© language and run on a personal computer. An evaluation was performed on a data set containing 12 images. The percent of tracked nerves (with respect to manual tracing) was on average 87%; the rate of false positive recognitions (with respect to total tracing) was on average 9%. Running times of the prototype were 4-5 minutes per image.**

## I. INTRODUCTION

The cornea is the external, transparent layer of the eye. It is approximately 500 $\mu$m thick and with three main layers, with two thin membranes in between: the epithelium on the external side, separated by the Bowman membrane from the thick, central stroma layer, followed by the Descemet membrane and finally the innermost endothelium layer. With a confocal corneal microscope, it is possible to acquire in a rapid and noninvasive way images from all these layers and membranes, e.g., to extract important clinical information on cornea state of health.

In particular, images collected from a specific depth inside endothelium, the subbasal layer, allow to visualize the nerve structures present in this area of the cornea. They are narrow and elongates structures lying flat inside a thin 10 $\mu$m layer (Fig. 1). These structures have been shown to be quite important to provide information about damages from surgical interventions on cornea (such as LASIK or PRK) or from prolonged contact lens wear [1]. More recently, a remarkable link has been shown between nerve tortuosity and the severity of diabetic neuropathy, one the most common and serious long term complications of diabetes [2].

At present, all these analyses are based on a tedious manual tracing of the nerves, e.g. [3], and thus the derived clinical parameter values are subjective and error prone. An automatic tool, capable of reliably extracting the nerve course and layout and to quantitatively measure e.g. their density or tortuosity, would provide a much easier, objective and clinically usable procedure. It would be thus expected to improve the reliability of derived clinical parameters and thus to enhance their diagnostic value in important pathologies such as keratoconus and diabetes. We will now report on our work for the development of such a tool.

Authors are with Department of Information Engineering, University of Padova, Via Gradenigo 6/A, 35131 Padova, Italy alfredo.ruggeri@unipd.it

## II. MATERIALS AND METHODS

Images of corneal subbasal epithelium were acquired in normal subjects with the ConfoScan 4 confocal microscope (Nidek Technologies, Italy). 12 images covering a field of 460x350 $\mu m$ were acquired at 40X magnification and saved as monochrome 768x576 pixel digital images .

In these images, nerves appear as bright linear structures lying over a darker background (Fig. 1(a)). Recognizing corneal nerves has thus some similarities with the vessel tracking task in retinal images. For this reason, our approach has been to start with the original algorithm we developed for the latter task [4] and then to modify it, also with the addition of new modules specifically aimed at the analysis of images of corneal subbasal epithelium.

### A. Pre-processing

Acquired images do not usually have a uniform luminosity and contrast, exhibiting darker areas in the peripheral regions of the image. This is due to many factors, including the spherical shape of corneal layers, which causes a non uniform reflection of illumination light in the different corneal areas, and the different attenuation of light along the various illumination paths. In order to compensate for this, a specific procedure, originally developed to normalize luminosity and contrast in retinal images [5], was applied. As this procedure increases the amplitude of noise, an averaging filter is then applied. In pre-processed images, the nerve structures appear definitely more visible even in the peripheral areas of the image (Fig. 1(b)).

### B. The original tracking algorithm

The algorithm (described in detail in [4]) starts by identifying a set of seeds points, to be used as starting points for the tracking procedure. A grid of equally-spaced rows and columns (one every 10 pixels) is analyzed by looking for variations in the gray level of pixels that may suggest an intersection with nerves. A detection threshold was empirically set at 0.66 times the average gray level on the whole image and all analyzed pixels exceeding this threshold are considered as seeds. Higher values of the threshold, which actually provided more seed points, did not provide better overall results.

Starting from each seed point, the tracking module moves along a nerve by drawing successive segments perpendicular to the nerve direction (cross-sections). Pixels on the cross-sections are classified with a fuzzy c-mean clustering applied

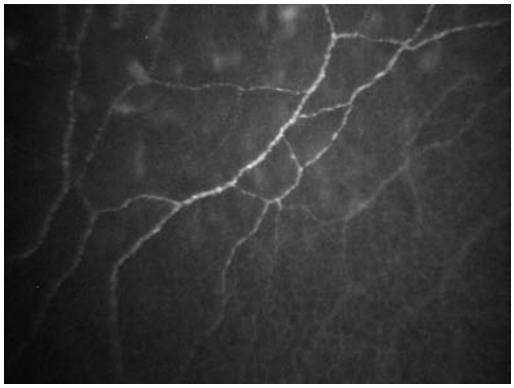

(a)

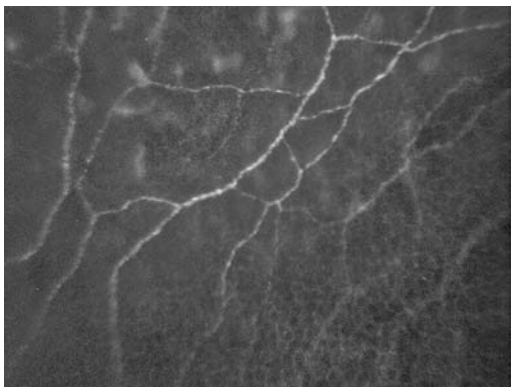

(b)

Fig. 1. Original (a) and pre-processed (b) images of sub-basal endothelium.

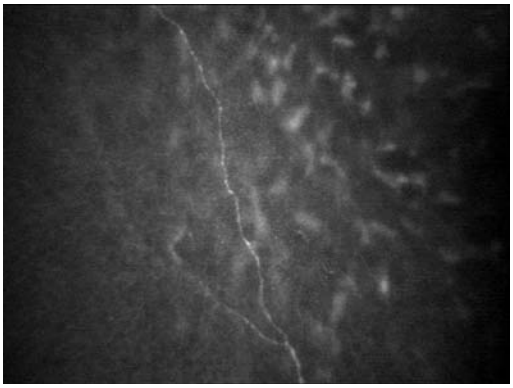

(a)

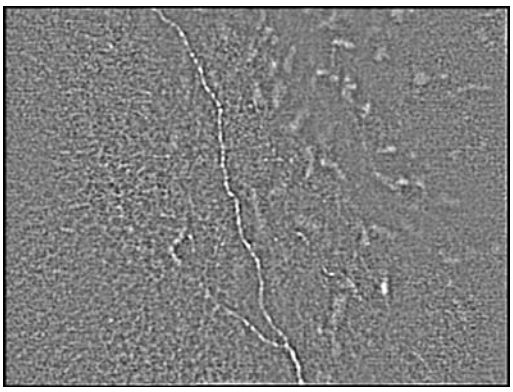

(b)

Fig. 2. Original (a) and high-pass filtered (b) images of sub-basal endothelium.

to their gray-levels, to obtain their classification into "nerve" and "non-nerve" pixels. A sequence of consecutive "nerve" pixels is interpreted as a nerve profile, whose width and spatial direction is determined.

The tracking strategy may result in the splitting of a single nerve into two or more segments, because of the presence of critical areas where the tracking algorithm has stopped. These segments belonging to the same nerve are likely to have end-points which face each other and that are likely to be similar with respect to direction, width and gray-scale intensity. In order to identify the end-point candidates to be connected, we have devised a greedy algorithm that decides whether to connect two end-points based on the values of the above mentioned features. In order to avoid a great deal of wrong connections of nerves with keratocytes cells (the white blobs appearing in the images), connection strategy was kept very conservative.

### *C. The new algorithm for tracking corneal nerves*

The results we obtained with the customized version of the retinal vessel tracking algorithms, described above, were reasonably good, but with wide space for improvements. The first one of such improvements was based on a high-pass filtered version of the acquired image, obtained by running a classical 3x3 derivative kernel (Fig. 2). Even at first glance, nerves appear much more visible on this latter image. The procedure is thus to perform nerve tracking as described in the preceding section and then, using the end-points of detected nerves, perform an additional tracking on the derivative image. This resulted in a higher percentage of correct nerves recognition, at the expenses of a slightly higher percentage of false recognitions. The whole issue of false nerve recognition will be dealt with later on (see below).

A second improvement was also aimed at increasing the rate of nerve recognition, in particular enhancing the connection between nerve segments. This is governed by the procedure described above. In order to boost the correct connections while at the same time limiting the false ones, we devised an additional strategy (see Fig. 3). Pairs of end-points candidates for connection are evaluated in a larger number than before and a more specific analysis is carried out. In each pair, five different arcs are drawn between the two end-points, simulating possible connections. The

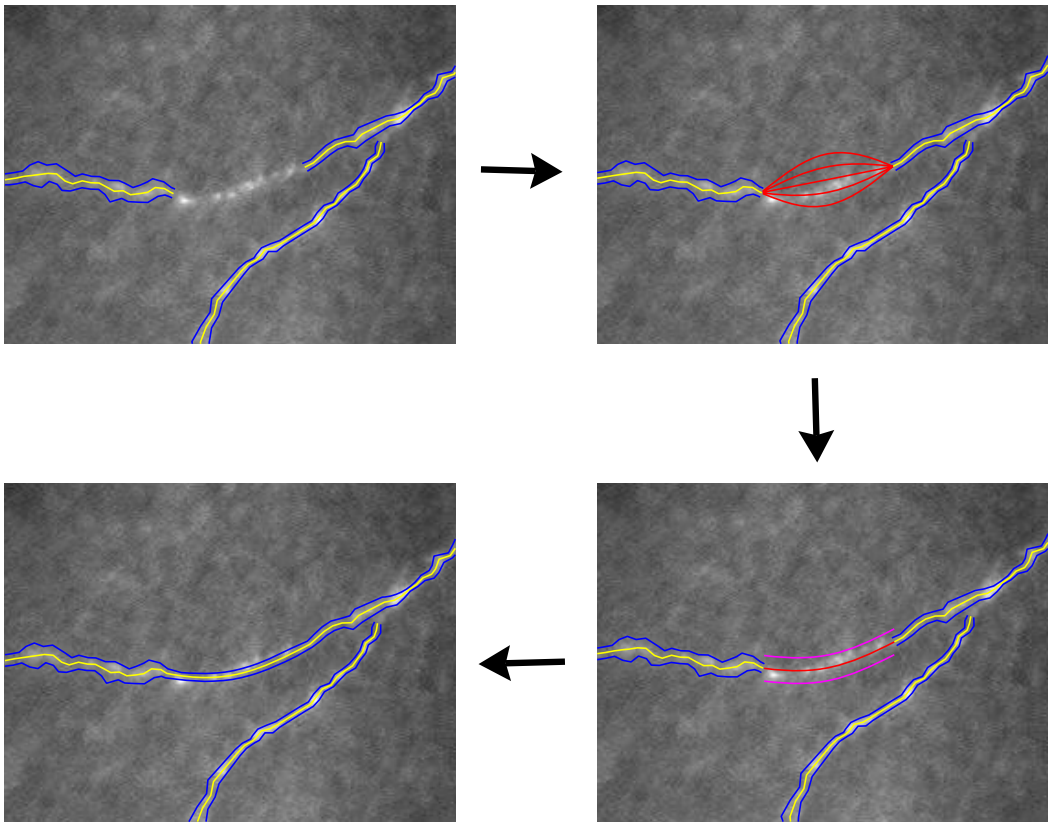

Fig. 3. The sequence of steps in the procedure to link two segments with arcs; yellow (blue) lines indicate nerve centerline (border), red lines indicate possible connections (see text).

one composed by pixels with the highest gray levels is selected as the most probable connection. Two more arcs (the "policemen") are then drawn, one on each side of the selected arc, at a predefined distance. If the difference between the gray levels of the selected arc and those of the "policemen" is larger than an empirically determined threshold, the selected arc is accepted as a true connection, otherwise it is rejected.

Improvements were also needed to reduce the number of false positive recognitions. The vast majority of these false recognitions were due to keratocytes being incorrectly identified as short segments of nerves. To quickly identify possible keratocytes, the original image was segmented by binarization and the resulting blobs were then morphologically dilated and eroded. In this image, white blobs represent either keratocytes or high-luminosity dots inside nerves. As recognized nerve segments inside the former should be deleted whereas the ones inside the latter should be confirmed, a specific procedure was developed. Short segments wholly contained inside white blobs were deleted (as they were assumed to be false recognitions inside keratocytes), whereas longer segments extending also outside white blobs were confirmed (as they were assumed to be true recognitions inside nerves).

Another technique that proved effective in eliminating many false recognitions was the analysis of the nerve width along single segments. True nerve segments are characterized by rather constant width values, whereas false recognitions usually have nerve width with many values larger than this constant value. Simply counting along each single segment the number of instances of width larger than an average value (10 pixel) allowed to detect many false recognitions, as they have this number larger than true nerve segments.

A prototype of the whole algorithm was implemented in the Matlab© language and run on a personal computer.

## III. RESULTS AND DISCUSSION

A preliminary evaluation was performed on the data set containing 12 images from normal subjects. At first, a manual detection of nerves was performed by tracing the nerves with a drawing software. The same images were then analyzed with the developed prototype, to provide the automatic detection. To smooth the derived nerve tracings, both manual

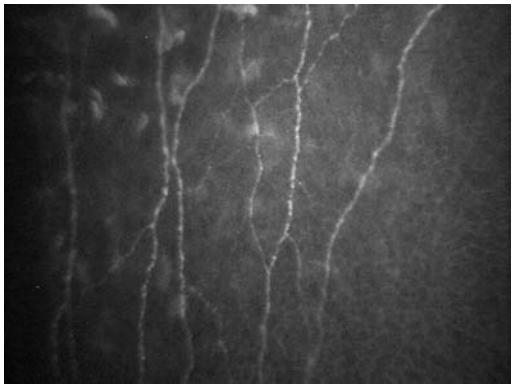

(a)

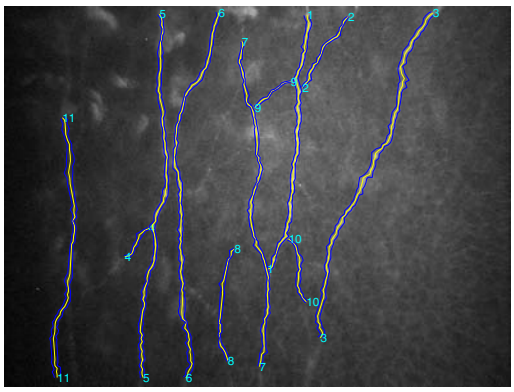

(b)

Fig. 4. Original image (a) and image with traced nerves (b); yellow (blue) lines indicate nerve centerline (border).

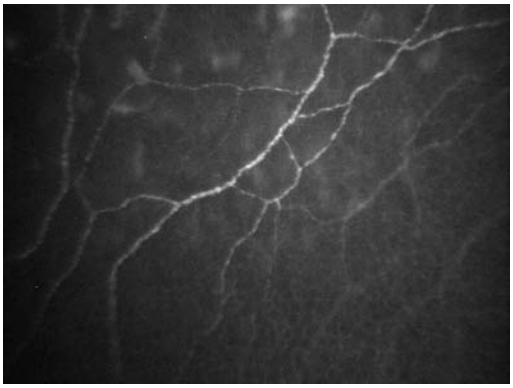

(a)

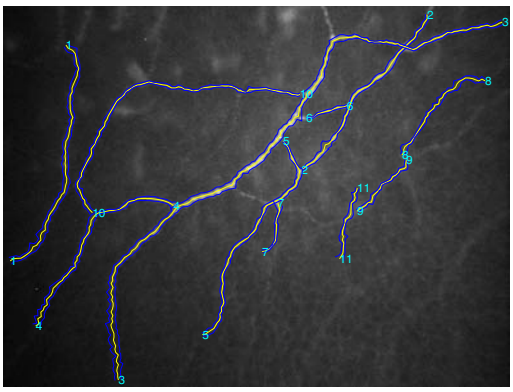

(b)

Fig. 5. Original image (a) and image with traced nerves (b); yellow (blue) lines indicate nerve centerline (border).

and automatic, a spline curve was fitted to them and length was measured on these smoothed profiles. The percent of nerve length tracked by the program (with respect to manual tracking) was on average 87.3% per image (range 51-100%), whereas the percent of false tracking (with respect to total tracked length) was on average 8.6% per image (range 0-21%). Running times of the prototype were 4-5 minutes per image. Two representative examples of the results obtained are shown in Fig. 4 and Fig. 5.

With the application of the algorithm presented here, important clinical parameters such as total length of nerves in the image, nerve density (length of nerve per $mm^2$), nerve tortuosity, could be derived in a easy, quantitative and objective way. A significant advantage on patient clinical assessment is reasonably expected, but is however still to be assessed, as it will require extensive clinical studies involving a great number of subjects, both normal and pathological. Moreover, clinical issues still to be considered are the balance between sensitivity and specificity of the nerve recognition and the acceptability of allowing some manual editing to improve them.

Implementation of the algorithm with a more efficient computer language, e.g. C++, will allow reducing execution time to a few tens of seconds.

## IV. Acknowledgments

The authors wish to thank Nidek Technologies Srl, Italy, for having kindly provided the ConfoScan 4 images.

## References

[1] S. Patel, J. McLaren, D.Hodge, and W. Bourne, "Confocal microscopy in vivo in corneas of long-term contact lens wearers," *Invest Ophthalmol Vis Sci*, vol. 43, pp. 995–1003, 2002.

[2] P. Kallinikos, M. Berhanu, C. O'Donnel, A. Boulton, N. Efron, and R. Malik, "Corneal nerve tortuosity in daibetic patients with neuropathy," *Invest Ophthalmol Vis Sci*, vol. 45, no. 2, pp. 418–422, 2004.

[3] L. Simo Mannion, C. Tromans, and C. O'Donnel, "An evaluation of corneal nerve morphology and function on moderate keratoconus," *Contact Lens Anterior Eye*, vol. 28, pp. 185–192, 2005.

[4] E. Grisan, A. Pesce, A. Giani, M. Foracchia, and A. Ruggeri., "A new tracking system for the robust extraction of retinal vessel structure," in *Proc. 26th Annual International Conference of IEEE-EMBS*, New York, 2004, pp. 1620–1623, IEEE.

[5] M. Foracchia, E. Grisan, and A. Ruggeri, "Luminosity and contrast normalization in retinal images," *Med Image Anal*, vol. 9, no. 3, pp. 179–190, 2005.